

See Online for webrable

Patient 2 was a 35-year-old Chinese man from China's Jiangxi province who had a 6-day history of fever and productive cough. He had participated in selling birds, of which several had died. On admission, chest radiographs showed evidence of pneumonia, and laboratory results showed abnormally increased hepatic-associated and cardiac-associated enzymes and lymphopenia. He was treated with antibiotics. Corticosteroids were given initially with methylprednisolone 40 mg on day 10 and then 120 mg per day for 17 days. Antiviral treatment was given, including rimantadine 100 mg twice daily on days 10 and 11 and then oseltamivir 150 mg per day from day 11 for 10 days. After admission, he became increasingly irritable and confused, followed by lowered consciousness. He developed respiratory failure and mechanical ventilation was initiated. In a sputum culture, several gram-positive microorganisms and *Candida albicans* were isolated. Antifungal drugs were added to his treatment. He developed multiple organ failure and died 27 days after the onset of symptoms.

The Chinese Centre for Disease Control and Prevention confirmed human infection with avian influenza H5N1 in both patients. RT-PCR detected H5N1 viral sequences in nasal swabs and nasopharyngeal aspirates, which were obtained on day 6 of illness for patient 1 and day 10 for patient 2. Viruses were isolated from the nasopharyngeal aspirate cultures, and designated as influenza A/Anhui/1/2005 virus¹⁸ in patient 1 and A/Jiangxi/1/2005 virus in patient 2. The haemagglutinin genes of viruses in patient 1 (GenBank accession number: DQ371928)¹⁸ and patient 2 (webappendix)¹⁹ were sequenced. The receptor-binding sites of both viruses were identical to those of previous H5N1 isolates.²⁰ H5N1 viruses isolated from both patients were susceptible to both the M2 inhibitors amantadine and rimantadine, and the neuraminidase inhibitors oseltamivir and zanamivir.

Both cadavers were stored at 4°C and underwent autopsy about 18–20 h after death. The autopsies were done following conventional protocols and strict safety procedures.²¹ Tissue samples from all major organs and tissues were taken and fixed in 4% formalin. The brain of patient 1 was not available for investigation.

Immunohistochemistry

Immunohistochemistry was done on the basis of the technique of Lin and colleagues, with antigen retrieval by a standard technique.^{22,23} To detect viral antigen, tissue slides of 4 µm thickness were incubated with mouse monoclonal antibodies to nucleoproteins and haemagglutinin. Furthermore, monoclonal antibodies to the following cell markers were used: CD68 (for macrophages), CD3 (T lymphocytes), CD20 (B lymphocytes), CD8 (cytotoxic T cells), S100 (dendritic cells), cytokeratin AE1/AE3 (epithelial cells), surfactant protein A (type II pneumocytes), tubulin-β (ciliated epithelial cells), placental alkaline phosphatase (PLAP, syncytiotrophoblasts), E-cadherin (cytotrophoblasts),²⁴

neurofilament (neurons), neuron-specific enolase (neurons), and factor VIII (endothelial cells, webrable).²⁵ For controls, we used unrelated antibodies in place of the primary antibody.

In-situ hybridisation

For the development of probes, we used haemagglutinin (GenBank accession number DQ100556) and nucleoprotein gene sequences (DQ100560) of the H5N1 A/black-headed gull/Qinghai/1/2005 virus, which was recently isolated from a migratory bird at China's Qinghai lake.²⁶ Plasmids were generated by cloning of the full haemagglutinin gene (1779 bp) and full nucleoprotein gene (1565 bp) into a plasmid vector pGEM-T (Promega, Madison, WI, USA) yielding pGEM-HA for haemagglutinin and pGEM-NP for nucleoprotein. Both plasmids were linearised with appropriate restriction enzymes. Two sense and two antisense RNA probes were prepared by in-vitro transcription with T7 and Sp6 RNA polymerase (Promega) in the presence of digoxigenin-UTP (Roche Diagnostics, Penzberg, Germany). Since H5N1 is a negative-stranded RNA virus, sense probes were defined as the probes that detect the viral RNA (negative-stranded); whereas antisense probes detected mRNA and complement RNA (cRNA), which are both positive-stranded.

Briefly, before hybridisation, all solutions were prepared with diethyl pyrocarbonate (DEPC)-treated water.²⁷ After deparaffinisation and rehydration, tissue sections of 4 µm thickness were treated with proteinase K digestion or microwave heating. Tissue sections were then incubated with a hybridisation cocktail containing 50 µg/ml of one of the four sense and antisense probes at 45°C for 16 h. All sense and antisense probes were applied separately on consecutive tissue sections. After blocking with horse serum (1:100), sections were incubated with alkaline phosphatase-labelled digoxigenin antibody (1:500, Roche Diagnostics, Penzberg, Germany) for 1 h, and the reaction products were colourised with nitroblue tetrazolium/5-bromo-4-chloro-3-indolyl phosphate (Promega).

As a positive control, we used brain tissue samples of a black-headed gull, for which H5N1 infection of the brain was confirmed by viral isolation.²⁸ We used lung tissues from a mouse infected with H9N2 influenza virus as a negative control. Negative controls also included an unrelated antisense probe against the fragment of the polymerase gene (RIAB) of the severe acute respiratory syndrome-associated coronavirus (SARS-CoV),²⁹ as well as H5N1 in-situ hybridisation probes to tissues (including lung and tracheal) obtained from seven adults who died from infectious lung diseases other than H5N1 influenza (four, SARS; one, purulent bronchitis; two, pneumonia), one adult who died from a non-infectious disease (gastric ulcer), one pregnant woman who died from an amniotic embolism, and one aborted fetus.

We identified the cell types infected by the virus with double labelling by combining in-situ hybridisation for

See Online for webappendix

viral genomic sequences and immunohistochemistry for one of the cell-associated markers. To identify placental cells and cerebral neurons containing viral sequences or antigens, consecutive sections adjacent to the sections used for in-situ hybridisation or immunohistochemistry were immunostained with CD68, E-cadherin, PLAP, neurofilament, or neuron-specific enolase. Tissues from the pharynx, nose and paranasal sinuses, and lymph nodes other than hilar nodes were not available for investigation.

On preliminary investigation of lung tissues, we noted a contrast between the extent of histological damage and the limited number of positive pneumocytes (patient 1) or absence of positive pneumocytes (patient 2) shown by in-situ hybridisation and immunohistochemistry studies. Therefore, we did extensive pulmonary sampling for further histological assessment to ensure that the results were representative.

Expected localisation of signals from in-situ hybridisation and immunohistochemistry

After receptor-mediated endocytosis of the virus, the polymerase proteins, nucleoprotein, and encapsidated RNA segments migrate to the nucleus of the infected cell. In the nucleus, RNA segments are transcribed into mRNA and cRNA. mRNA is subsequently translated to viral proteins (eg, haemagglutinin and nucleoprotein) in the cytoplasm. Newly synthesised nucleoprotein is transported back to the nucleus. cRNAs function as

antigenomic templates for the production of progeny RNA segments in the nucleus. Assembly of progeny gene segments and proteins occurs in the cytoplasm.⁴

Therefore, sense and antisense signals after in-situ hybridisation for nucleoprotein and haemagglutinin could be seen in both the nucleus and cytoplasm of infected cells, as well as immunohistochemical signals for nucleoprotein in the nucleus and for haemagglutinin in the cytoplasm. Since antisense probes hybridise to mRNA and cRNA, a positive signal would probably indicate active viral replication.

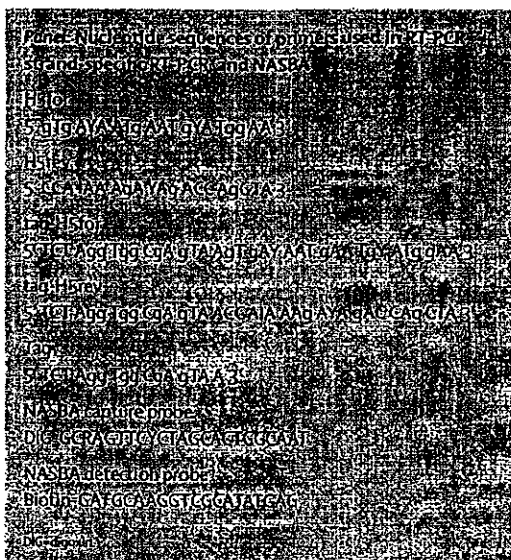
RT-PCR, real-time RT-PCR, and NASBA

RNA was extracted from deparaffinised tissue samples, or directly extracted from formalin-fixed tissues after overnight incubation with proteinase K (10 µg/µL, Amersco, Cleveland, OH, USA). We did RNA extraction with Trizol (Invitrogen, CA, USA), and PCR as previously described.²¹ The haemagglutinin gene of the H5N1 virus was detected with H5for as the forward primer and H5rev as the reverse primer for H5 gene amplification (panel). Reamplification was done for specific samples with the same set of primers if no band was seen in gel electrophoresis. We obtained negative controls for RT-PCR from uninfected tissues (eg, lung, brain, placenta; and intestine) from three patients who died from non-infectious diseases. RT-PCR for glyceraldehyde-3-phosphate dehydrogenase (GAPDH) was assessed in parallel as an internal control.

To detect viral RNA in fetal tissues, real-time RT-PCR (H5 avian influenza virus Nucleic Acid Amplification Fluorescent Quantitative Detection Kit, PG Biotech, Shenzhen, China) was used as recommended by the manufacturer and the national standards of the People's Republic of China.

Trachea	-/+	-/+	-/+	-/+	+/+	+/+
Bronchi	-/+	-/+	-/+	-/+	+/+	+/+
Lymph nodes	+/+	-	+/+	+/+	-	-
Heart	-/+	-/+	-/+	-/+	-/+	-/+
Prostate gland	-/+	-/+	-/+	-/+	-/+	-/+
Hepatocytes	-/+	-/+	-/+	-/+	-/+	-
Kidneys	-/+	-/+	-/+	-/+	-/+	-
Small intestine	-/+	-/+	-/+	-/+	-/+	-/+
Brain	-	-	+/+	+/+	-	-
Synytiotrophoblasts	-/+	-/+	-/+	-/+	n/a	n/a
Cytotrophoblasts	+/+	+/+	n/a	n/a	n/a	n/a
Circulating mononuclear cells	-/+	-/+	-/+	+/+	+/+	+/+

Table 1. Results of the in-situ hybridisation and immunohistochemistry in selected organs and cell types.



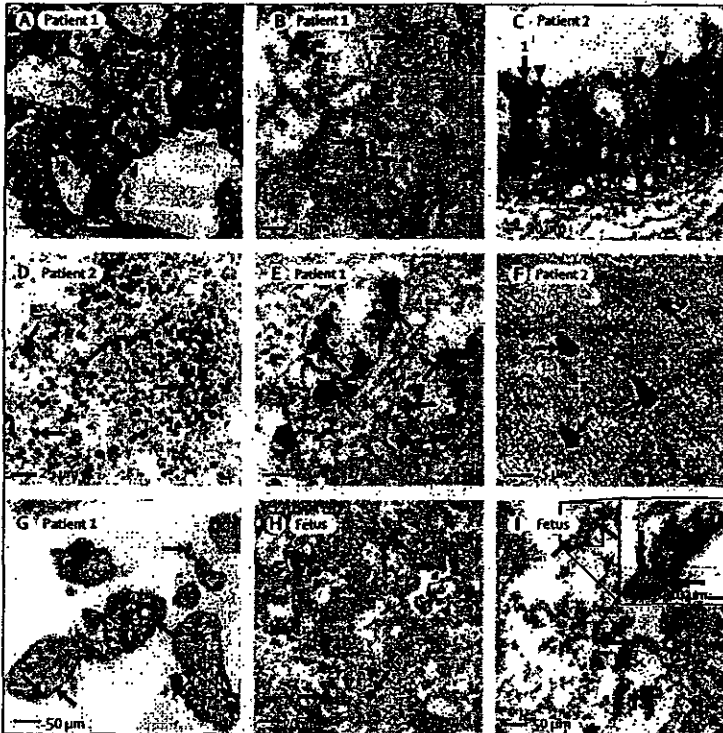


Figure 1: In-situ hybridisation locating gene sequences of H5N1 viral antigens (nucleoprotein and haemagglutinin)

Signals seen with nitroblue tetrazolium/5-bromo-4-chloro-3-indolyl phosphate (purple-blue) and immunohistochemical signals with 3-amino-9-ethylcarbazole (double labelling, brown-red). No counterstaining done unless stated otherwise. (A) Lung tissue showing severe damage, hyaline membrane formation, and oedema (by haematoxylin and eosin staining), by contrast with limited number of cells positive for in-situ hybridisation in lung tissue of patient 1 (figure 1B). (B) Positive signals (with nucleoprotein sense probe) in nuclei of isolated pneumocytes (arrows). (C) Double labelling of in-situ hybridisation (with nucleoprotein antisense probe) and immunohistochemistry (with tubulin- β antibody; brown, arrowheads) showing dark-blue viral genomic sequences (arrows) in cytoplasm of tubulin-negative non-ciliated cell (arrow 1) and tubulin-positive ciliated cell (arrow 2) in trachea. No signal seen in nuclei (lightly counterstained with methyl-green). (D) Positive signals (with nucleoprotein sense probe) in several mononuclear cells in lymph node (arrows, lightly counterstained with methyl-green). (E) Positive signals (with nucleoprotein antisense probe) in mucosal epithelial cells of small intestine (arrows, lightly counterstained with methyl-green). (F) Positive signals (with nucleoprotein sense probe) in brain cells (arrows) from left parietal lobe (lightly counterstained with methyl-green), mainly located in cytoplasm and confirmed to be neurons from immunostaining for neurofilament or neuron-specific enolase (webfigures 2O and 2P). (G) Positive signals (with nucleoprotein antisense probe) in large mononuclear cells with morphological features of cytotrophoblasts in periphery of chorionic villus (arrows). Cells confirmed as cytotrophoblasts (webfigure 4D). No positive signals noted in any syncytiotrophoblasts. (H) Positive signals (with nucleoprotein sense probe) in fetal liver cells (arrows), confirmed as Kupffer cells (webfigure 1F). (I) Positive signals (with haemagglutinin sense probe) in bronchiolar epithelial cells in fetal lung tissue (arrows).

Strand-specific RT-PCR was undertaken on the basis of the technique of Yue and co-workers,²¹ with minor modification. Briefly, two-part reactions were used. First, the RT reaction was done in the presence of tagged primer, tag-H5for or tag-H5rev (panel). A third of cDNA products then underwent PCR with primers Tag/H5rev or Tag/H5for. We reamplified under the same PCR conditions for a specific sample if no band was seen after gel analysis of the first PCR reaction.

Virus-specific RNA was also detected with the avian influenza virus (H5 subtype) NASBA diagnostic test kit

(MP version, Hong Kong DNA Chips, Hong Kong). The test was done as previously described²² with H5-specific capture and detection probes (panel). Absorbance of the amplified product was measured at 405 nm by an ELISA plate reader (Bio-Rad, Hercules, CA, USA). A negative control from the test kit was also included for H5 detection. The study was approved by the internal review board and ethics committee of the Peking University Health Science Centre.

Role of the funding source

The sponsor of the study had no role in study design, data collection, data analysis, data interpretation, or writing of the report. The corresponding author had full access to all the data in the study and had final responsibility for the decision to submit for publication.

Results

The microscopic features of both patients were similar, apart from more extensive fibroproliferative changes in the lungs of patient 2. Both lungs of patient 1 showed features of diffuse alveolar damage (figure 1A) and focal desquamation of epithelial cells into alveolar spaces without evidence of type II pneumocyte hyperplasia. In the lungs of patient 2, patchy foci of consolidated bronchopneumonia and areas of fibrosis were seen. We found variable numbers of macrophages in the alveoli (especially in patient 2), and moderate numbers of scattered neutrophils and rare lymphocytes in the interstitial spaces. Both patients had substantially depleted lymphoid tissue in the spleen, lymph nodes, and mucosal lymphoid tissue in the gastrointestinal tract. The liver in both patients had spotty necrosis. In both patients, we detected very low numbers of macrophages with haemophagocytosis in the spleen, lymph nodes, and liver. The kidneys showed extensive tubular necrosis. Other organ systems showed no pronounced histological changes, apart from hypertrophy in the thymus of patient 2.

The placenta showed development appropriate for the length of gestation. We saw scattered foci of syncytiotrophoblast necrosis, sometimes with associated dystrophic calcification. Whether this finding was induced virally or was the sole result of maternal shock is unclear. Acute necrotising deciduitis was detected focally, and regarded as consistent with maternal shock.

Fetal tissues mostly showed no specific histopathological findings, and development was also consistent with gestational age. However, sections of fetal lung showed oedema and very small numbers of scattered interstitial neutrophils, which raised the possibility of mild acute interstitial pneumonitis, although this appearance was notably less severe than that seen in patients 1 and 2 (webfigure 1).

Sense and antisense probes for in-situ hybridisation detected viral genomes focally in tissue samples from various organs (table 1). The two sets of probes (for

See Online for webfigure 1

haemagglutinin and nucleoprotein) generated identical staining results. In both autopsies, the trachea, small intestines, and lymph nodes showed positive signals of in-situ hybridisation, although pneumocytes were positive only in patient 1. In the lungs, sense probes hybridised in the nuclei of pneumocytes (figure 1B), whereas antisense probes hybridised in both the cytoplasm and nuclei. In all other organs with positive signals, both sense and antisense were present mainly in the cytoplasm of infected cells.

In the respiratory tract, we detected positive signals in tracheal epithelial cells and alveolar epithelial cells (figures 1B and 1C, webfigure 1). However, only an estimated 10–20% of epithelial cells in the trachea and about 5% of epithelial cells in the alveoli showed positive signals. Both bronchi and bronchioles were negative. Double labelling combining in-situ hybridisation and immunohistochemistry with tubulin-β antibody showed that both ciliated (tubulin-β-positive) cells and non-ciliated (tubulin-β-negative) cells of the trachea had viral sequences (figure 1C, webfigure 2). We also found putative basal cells to be infected. Double labelling with antibodies for cytokeratin and surfactant protein A showed that the positive alveolar cells were type II pneumocytes (webfigures 1C and 1D). In-situ hybridisation showed no positive staining in endothelial cells, macrophages, lymphocytes, fibroblasts, or any other cell type in the lungs or blood. However, we found positive viral signals in the cytoplasm of mononuclear cells in hilar lymph nodes (figure 1D). Double labelling and consecutive sections showed that cells positive for in-situ hybridisation were T lymphocytes (ie, positive for CD3 and negative for CD68, CD20, and S100, webfigure 3). Additionally, positive signals of intracytoplasmic viral sequences were present in mucosal epithelial cells of the

small intestine (>50% in some intestinal segments, figure 1E). We also detected viral sequences in the cytoplasm (and to a much lesser extent in the nuclei) of brain cells from patient 2 (figure 1F, webfigure 1). Double labelling with neural markers neurofilament or neuron-specific enolase showed that these H5N1-positive cells were neurons (webfigures 1O and 1P). Table 2 shows the topographic distribution of cells with positive signals from in-situ hybridisation. No positive signals were seen in the heart, liver, spleen, kidneys, oesophagus, bone marrow, or stomach.

Placental tissue samples showed a large number of infected cells in chorionic villi (webfigure 4). Most positive cells were localised in the connective tissue core of these villi. These cells were confirmed (by labelling with monoclonal antibodies to CD68 and PLAP in consecutive sections) to be Hofbauer cells but not syncytiotrophoblasts. A subgroup of the cells with positive signals was found in the periphery of chorionic villi (figure 1G), which morphologically resembled cytotrophoblastic cells and were confirmed by immunostaining with E-cadherin antibody on consecutive sections. No positive signal was seen in syncytiotrophoblasts.

In the fetus, in-situ hybridisation identified viral sequences in the lungs, circulating mononuclear cells (webfigure 1), and mononuclear cells in the liver (figure 1H). The latter cells were identified as macrophages (Kupffer cells) by double labelling with antibody to CD68 (webfigure 1). Both sense and antisense probes were

See Online for webfigures 2, 3, and 4.

Organ	Signal	Count
Frontal lobe	+	2499
Occipital lobe	+	2312
Temporal lobe	+	2466
Thalamus	+	2295
Mesencephalon	+	2190
Pons	+	2031

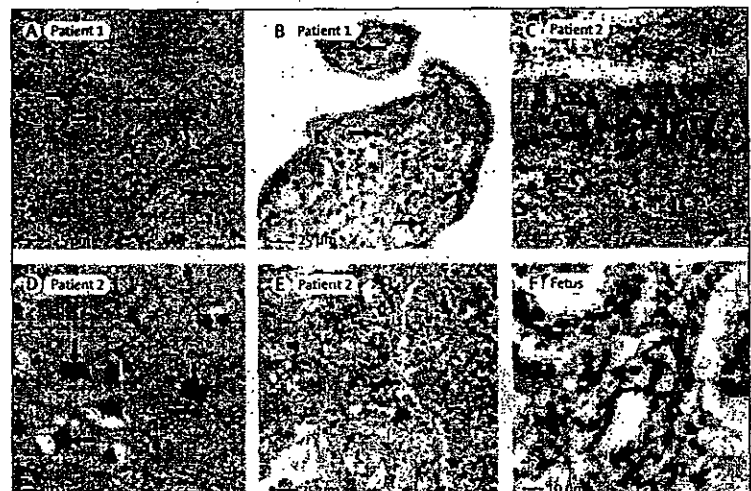


Figure 2: Immunohistochemical staining for H5N1 viral antigens (nucleoprotein, haemagglutinin). Positive signals seen with diaminobenzidine (brown; Zymed Laboratories, San Francisco, CA, USA) or 3-amino-9-ethylcarbazole (red-brown; Sigma, St Louis, MO, USA). Slides counterstained with haematoxylin. (A) Positive staining (with nucleoprotein antibody) in nuclei and cytoplasm of pneumocytes (arrows). (B) Positive signals (with nucleoprotein antibody) in nuclei of mononuclear cells (arrows) with morphological features of macrophages in core of chorionic villus. Immunostaining in adjacent sections indicate cells to be Hofbauer cells (webfigure 4). (C) Positive signals (with nucleoprotein antibody) in nuclei of epithelial cells of trachea (arrows). (D) Positive staining (with nucleoprotein antibody) in cytoplasm and nuclei of neurons (arrows) from hippocampus. (E) Positive staining (with haemagglutinin antibody) in mononuclear cell in lymph node (arrow). (F) Positive staining (with haemagglutinin antibody) in cytoplasm of pneumocytes (arrows) in fetal lung tissue.

positive, mainly in the nuclei of pneumocytes and in a few detached epithelial cells of the bronchi (figure 11). In Kupffer cells and circulating mononuclear cells, sense and antisense probes showed positive signals in both the cytoplasm and nucleus. The fetal lungs appeared to have more positively stained cells than did the maternal lungs.

The specificity of in-situ hybridisation was established by the results with the negative and positive controls (webfigure 1). The brain sections of the black-headed gull showed almost all neurons with positive signals for in-situ hybridisation, indicating the high detecting sensitivity of this technique.

Distribution of immunohistochemical staining (table 1) was consistent with that of in-situ hybridisation, apart from the absence of viral antigens in the intestines. Positive staining for nucleoprotein and haemagglutinin

was detected in pneumocytes (figure 2A) and cytotrophoblasts and Hofbauer cells in the placenta (figure 2B) in patient 1; as well as in tracheal epithelial cells (figure 2C), the brain (figure 2D), and T lymphocytes in hilar lymph-node tissue (figure 2E) in patient 2. The fetus showed positive staining in bronchial epithelial cells, pneumocytes (figure 2F), and circulating mononuclear cells. Nucleoprotein was mainly detected in the nucleus and haemagglutinin in the cytoplasm. Negative controls validated the specificity of the immunohistochemistry protocol (webfigure 5).

All organs tested showed positive RT-PCR results, apart from the lymph nodes of patient 2 (tables 2 and 3, figure 3). All non-paraffin-embedded samples were positive for H5 expression. However, paraffin-embedded tissues only showed H5 expression after reamplification of the RT-PCR products. NASBA showed positive results on both types of samples without the need of reamplification.

With real-time RT-PCR, viral RNA was detected in the lungs and liver of the fetus (table 3). GAPDH was an internal control for successful RNA extraction in these assays. Positive-stranded RNA was detected in the heart and placenta of patient 1 and in the lungs, trachea, intestines, and brain of patient 2 (table 3, figure 3). The specificities of the RT-PCR and NASBA were further confirmed by use of the negative controls.

Discussion

Our comprehensive investigation of the tissue tropism of H5N1 influenza virus, based on two adult autopsies and one fetal autopsy, focuses on the localisation of viral genomic sequences and antigens. We present evidence suggesting that the virus disseminates beyond the respiratory system. In addition to the lungs, viral sequences and antigens were found in the cerebral neurons and lymphocytes.

Presence of viral sequences and antigens in the CNS is consistent with the recent isolation of H5N1 virus from cerebrospinal fluid of a boy who died from encephalitis⁴ with neurological symptoms commonly seen in patients with H5N1 influenza (Gao Zh, unpublished), including the two cases in this study. Brain neurons were found to be infected by the virus. We also saw regional variations in positive neuronal distribution and negative neurons next to positive neurons. Possible reasons might include differing densities of the avian influenza virus receptor in human beings, differences in blood supply pathways and nerve connections that allow virus-target cell contact, and differing viral loads and viral replication stages. The detection of positive-stranded RNA by RT-PCR and in-situ hybridisation could indicate active viral replication in the brain. The virus could reach the CNS by penetrating the blood-brain barrier or by invading the afferent fibres of the olfactory, vagal, trigeminal, and sympathetic nerves after replicating in the respiratory mucosa, as has been shown in animals.²⁴

See Online for webfigure S

Trachea	-	-	-	Y	Y	Y	-	-	n/a	1-236	Y
Brain	-	-	-	Y	Y	Y	-	-	n/a	2-424	Y
Spleen	Y	Y	N	Y	N	N	-	-	1-326	Y	1-442
Kidneys	Y	Y	N	Y	N	N	N	-	2-371	Y	1-587
Placenta	Y	Y	Y	n/a	n/a	n/a	n/a	-	1-653	Y	n/a

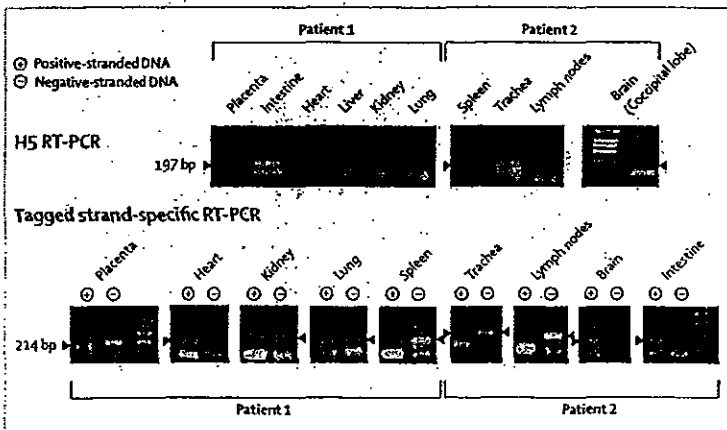


Figure 3: H5 RT-PCR and tagged strand-specific RT-PCR on selected organs. No positive band in RT-PCR seen for lymph nodes in patient 2.